

# Phase-sensitive optical low-coherence reflectometry for the detection of analyte concentrations

Kirill V. Larin, Taner Akkin, Rinat O. Esenaliev, Massoud Motamedi, and Thomas E. Milner

Optical techniques may potentially be used for noninvasive glucose sensing. We investigated the application of phase-sensitive optical low-coherence reflectometry (PS-OLCR) to the measurement of analyte concentrations. The dependence of the PS-OLCR signal on the concentration of various analytes, including aqueous solutions of glucose, calcium chloride, magnesium chloride, sodium chloride, potassium chloride, potassium bicarbonate, urea, bovine serum albumin, and bovine globulin, were determined in clear and turbid media. Obtained results demonstrated (1) a high degree of sensitivity and accuracy of the phase measurements of analyte concentrations with PS-OLCR; (2) a concentration-dependent change in the phase-shift for glucose that is significantly greater than that of other analytes sampled over the same physiological range; and (3) a high submillimolar sensitivity of PS-OLCR for the measurement of glucose concentration. Further exploration of the application of PS-OLCR to the noninvasive, sensitive, and specific monitoring of glucose concentration seems warranted. © 2004 Optical Society of America

OCIS codes: 110.4500, 120.5050, 170.1470, 170.4580.

## 1. Introduction

Noninvasive measurement and quantification of analytes are important for many biological, environmental, chemical, and clinical sciences. The refractive index is a fundamental optical property of a medium. The detection of small changes in the refractive index is often required for optical monitoring or diagnostics. Currently used refractometric systems are limited to the study of clear or near-clear media and are unsuitable for noninvasive assessments of tissues. Therefore a great demand exists for the development of an accurate and noninvasive technique that is capable of detecting ultrasmall fluctuations of the refractive index in tissue.

Since the introduction of optical coherence tomog-

raphy (OCT) in 1991,<sup>1</sup> significant progress has been achieved in the development and deployment of OCT for imaging and, more recently, optical monitoring. The OCT technique has several advantages over other optical methods, including high resolution ( $\leq 10 \mu\text{m}$ ), layer-specific probing capabilities, high dynamic range ( $>100 \text{ dB}$ ), and noninvasive measurement capability. A review of recent significant achievements in the development of OCT and OCT-based systems and their biomedical and nonbiomedical applications can be found in Refs. 2 and 3.

Differential phase-contrast optical coherence tomography (DP-OCT) was recently introduced in a bulk optics system by Hitzenberger and Fercher<sup>4</sup> and in a fiber interferometer by Davé and Milner.<sup>5</sup> Although conventional OCT is based on the detection and analysis of the intensity of backscattered optical radiation, DP-OCT utilizes the phase information obtained by probing a sample simultaneously with two common-path low-coherence beams. Variations in the sample refractive index are reflected in the phase difference,  $\Delta\phi$ , between these two beams. The DP-OCT technique is capable of measuring angstrom-nanometer-scale path-length changes between the beams [associated with the phase difference as  $\Delta p = (\lambda/4\pi) \Delta\phi$ ] in clear and scattering media.<sup>6,7</sup>

The highly sensitive and accurate noninvasive detection of analyte concentration in turbid media is

---

K. V. Larin and R. O. Esenaliev are with the Laboratory for Optical Sensing and Monitoring, The University of Texas Medical Branch, Galveston, Texas 77555. They, along with M. Motamedi, are also with the Center for Biomedical Engineering, The University of Texas Medical Branch, Galveston, Texas 77555. T. Akkin and T. E. Milner (milner@mail.utexas.edu) are with the Department of Biomedical Engineering, The University of Texas at Austin, Austin, Texas 78712.

Received 17 November 2003; revised manuscript received 23 March 2004; accepted 29 March 2004.

0003-6935/04/173408-07\$15.00/0

© 2004 Optical Society of America

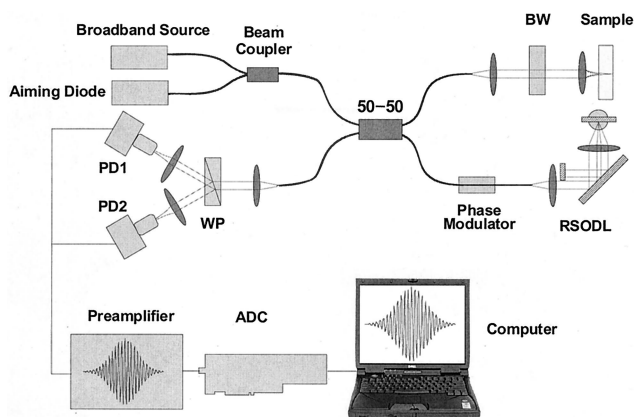


Fig. 1. Schematic of the PM fiber-based dual-channel PS-OLCR used in this study: BW, birefringent wedges; PD1 and PD2, photodetectors; WP, Wollaston prism; RSODL, rapid-scanning optical delay line; and ADC, analog-to-digital converter.

particularly relevant to the development of a blood glucose biosensor. Recently we applied a conventional OCT technique to noninvasive monitoring of blood glucose concentration by probing the skin of animals and humans.<sup>8,9</sup> In those studies we monitored changes in tissue scattering as a function of blood glucose concentration (variation of glucose concentration in the extracellular space produces changes in the refractive-index mismatch between the extracellular fluid and the scattering centers and, therefore, affects the tissue scattering properties). We also experimentally and theoretically studied several aspects of the specificity of the noninvasive monitoring of glucose concentration in tissues by using the OCT technique.<sup>10</sup> Despite these results, the concentration-dependent effect of glucose and other tissue analytes on the refractive index in the near-infrared (NIR) spectral range at physiological concentrations requires additional study with a more sensitive method.

In this paper we present results of a pilot study on the application of novel polarization-maintaining (PM) fiber-based dual-channel phase-sensitive optical low-coherence reflectometer (PS-OLCR) for the highly sensitive detection of analyte concentration in clear and turbid tissue phantoms. We studied the concentration-dependent effect on the phase shift and refractive index of aqueous solutions of D-glucose ( $C_6H_{12}O_6$ ), calcium chloride ( $CaCl_2$ ), magnesium chloride ( $MgCl_2$ ), sodium chloride ( $NaCl$ ), potassium chloride ( $KCl$ ), potassium bicarbonate ( $KHCO_3$ ), urea, bovine serum albumin (BSA), and bovine  $\gamma$ -globulin.

## 2. Materials and Methods

### A. Experimental Setup

Figure 1 shows a schematic of the PM fiber-based dual-channel PS-OLCR used in this study. A more detailed description of the system design and operation can be found in Ref. 11. Briefly, light emitted from a broadband light source (optical semiconductor

amplifier, AFC Technologies Incorporated; central wavelength  $\lambda_0 = 1.31 \mu\text{m}$ , bandwidth  $\Delta\lambda \approx 60 \text{ nm}$ ) was combined with an aiming beam from a laser diode ( $\lambda \approx 640 \text{ nm}$ ) and delivered to a 50–50 beam splitter in two independent linearly polarized modes that propagated along the birefringent axes of the PM fiber. Light returned from the sample arm and light reflected from the reference arm formed an interferogram, which was delivered to the detection arm of the interferometer. The birefringent wedges (Karl Lambrecht Corporation, Chicago, Illinois) in the sample arm were used to introduce a path-length delay between the two linearly polarized modes. By adjusting the thickness of the prisms, simultaneous signals were obtained from the front and back surfaces of glass cells (Friedrich & Dimmock Incorporated, Millville, New Jersey) with an inner thickness of approximately  $485 \mu\text{m}$ . The rapid-scanning optical delay line (RSODL)<sup>12</sup> in the reference arm was configured to compensate for the material and waveguide dispersion introduced by the  $LiNbO_3$  phase modulator. The phase modulator was driven with a ramp waveform with a voltage amplitude that gave a  $2\pi$  phase modulation and produced a pure sinusoid. The polarization channels in the detection arms were separated by use of a 20-deg Wollaston prism (Karl Lambrecht Corporation, Chicago, Illinois) and were captured by photoreceivers (New Focus, Incorporated, San Jose, California). The signal from each photoreceiver was filtered, amplified, and delivered to a personal computer for further processing with an analog-to-digital converter.

Several experiments were performed with a white-light refractometer (Bausch & Lomb, Rochester, New York). Absolute values of the refractive-index change were measured as a function of concentration for several analytes and were compared with reference data from the literature.

### B. Signal Processing

Processing of PS-OLCR signals was completed by use of MATLAB 6.0 software. To extract the phase difference between the two channels, the interference fringe signals were denoised with a type-II Chebyshev band-pass filter, which is monotonic in the passband. Forward and reverse filtering provided zero-phase distortion. The Hilbert transform of the signal was calculated to obtain the phase. Phases were unwrapped to remove jumps, and subtraction of the two channels yielded the phase difference,  $\Delta\phi$ .

### C. Phantoms

Aqueous solutions of D-glucose,  $CaCl_2$ ,  $MgCl_2$ ,  $NaCl$ ,  $KCl$ ,  $KHCO_3$ , urea, BSA, and bovine  $\gamma$ -globulin were used in this study. All the chemicals were obtained from Sigma-Aldrich Chemical Corp (Bellefonte, Pennsylvania). Aqueous solutions of different concentrations were prepared by dilution of the stock chemicals with pure water.

Several experiments were performed with aqueous suspensions of polystyrene microspheres (Bangs Laboratories, Incorporated, Fishers, Indiana). The mi-

crosspheres were chosen to simulate tissue scattering in phantom studies because of the stability of their optical properties and the simplicity of the theoretical calculations of the scattering coefficient (e.g., using the Mie theory of scattering).<sup>13,14</sup> Polystyrene spheres (760-nm diameter) have strong scattering and negligible absorption in the NIR spectral range and are widely used to simulate tissue scattering.<sup>15–17</sup> Several phantoms with the same concentration of polystyrene microspheres and different concentrations of D-glucose were used in the experiments. The sphere concentrations were chosen to provide scattering coefficients  $\mu_s \cong 50$  and  $100 \text{ cm}^{-1}$  at  $\lambda = 1.31 \text{ }\mu\text{m}$  (typical for tissues in the NIR spectral range).

Samples were placed in a glass cell, and the incident beam from the PS-OLCR system was directed perpendicular to the cell wall. Five independent measurements of  $\Delta\phi$  were performed for each analyte concentration and for pure water. The time interval between the measurements was 1–2 min. The phase shift corresponding to each analyte concentration was calculated as  $\Delta\phi = \Delta\phi_{\text{analyte}} - \Delta\phi_{\text{water}}$  (in the case of experiments with polystyrene microspheres, the phase shift of each analyte concentration was calculated as  $\Delta\phi = \Delta\phi_{\text{ps+analyte}} - \Delta\phi_{\text{ps}}$ , where “ps” stands for the aqueous suspensions of polystyrene microspheres). The experiments were performed with two to five sets of the suspensions that were independently prepared. The standard deviation (SD) was calculated for each data point, based on five measurements of the same concentration.

### 3. Results

Figure 2 shows the refractive indices of aqueous solutions of glucose, NaCl, urea, and BSA as a function of the concentration obtained from the refractometer study. Six concentrations from 0 to 100 mM were measured and plotted as scatters, together with the SD for each data point. The data extrapolated from the literature for the sodium D line ( $\lambda = 589 \text{ nm}$ )<sup>18</sup> are plotted as solid, dashed, and dotted lines for glucose, NaCl, and urea, respectively [Fig. 2(a)]. The data extrapolated from the literature for  $\lambda = 436 \text{ nm}$ <sup>19</sup> are plotted as a solid line for BSA in Fig. 2(b). These data show generally good agreement between the refractive indices measured in the white-light refractometer study and those previously reported in the literature for wavelengths in the visible spectral range.

Figure 3 shows the dependence of the phase shift on the concentration of glucose,  $\text{CaCl}_2$ ,  $\text{MgCl}_2$ , NaCl, KCl,  $\text{KHCO}_3$ , urea, BSA, and globulin obtained in the PS-OLCR study in the clear media (shown as squares with the SD bars). The refractive-index dependence on the analyte concentration for the visible spectral range reported in the literature<sup>18,19</sup> was used to calculate the phase-shift dependencies on the concentrations (shown as the solid line). Linear fitting of experimental PS-OLCR data points (not shown) by use of a linear least-squares algorithm yielded a correlation coefficient better than 0.99 and a *P* value less than 0.01% for all analytes studied. From these re-

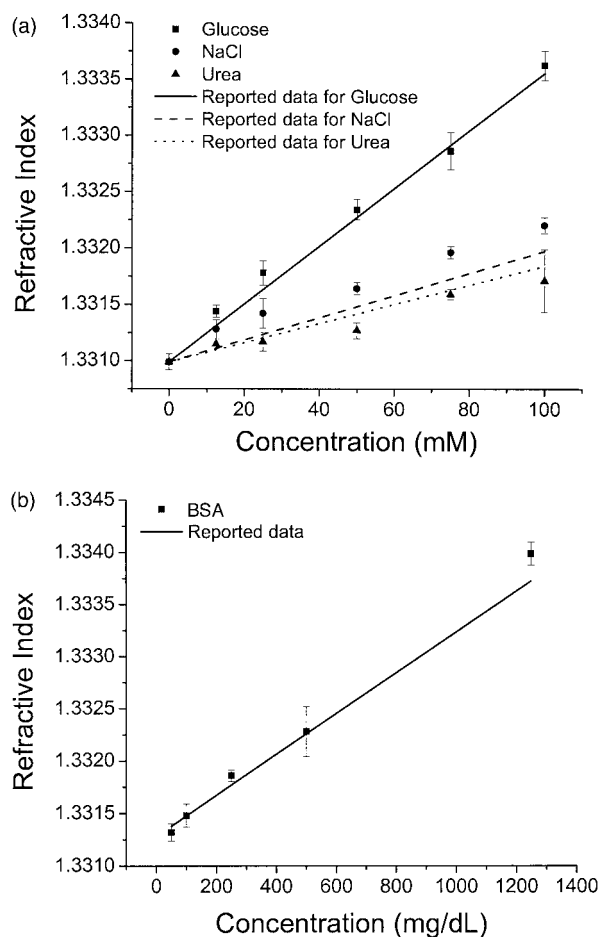


Fig. 2. Refractive index versus analyte concentration obtained from the white-light refractometer study and from the literature for (a) glucose, NaCl, and urea and (b) BSA.

sults we note that (1) a good linear correlation exists between the increase of analyte concentration and the PS-OLCR phase shift and (2) the effect of the phase-shift increment with increasing analyte concentration is similar or slightly less in the NIR than in the visible spectral range.

Several experiments were performed using turbid media with a scattering coefficient similar to that of human tissues in the NIR spectral range. Figure 4 presents a typical dependence of the phase shift on glucose concentration in an aqueous suspension of polystyrene microspheres of fixed concentrations. The scattering coefficients of the two phantoms were  $50$  and  $100 \text{ cm}^{-1}$  [Figs. 4(a) and 4(b), respectively]. The concentrations of polystyrene microspheres were chosen according to the calculations performed on the basis of Mie scattering theory<sup>13,14</sup> and were equal to 0.8% and 1.6% (w/w) for  $\mu_s = 50 \text{ cm}^{-1}$  and  $\mu_s = 100 \text{ cm}^{-1}$ , respectively. Five glucose concentrations in the range 20–100 mM with a 20-mM increment were measured in these experiments. The results obtained were similar to those found in clear-media studies (solid line), suggesting the applicability of this technique to the sensing and monitoring of turbid samples.

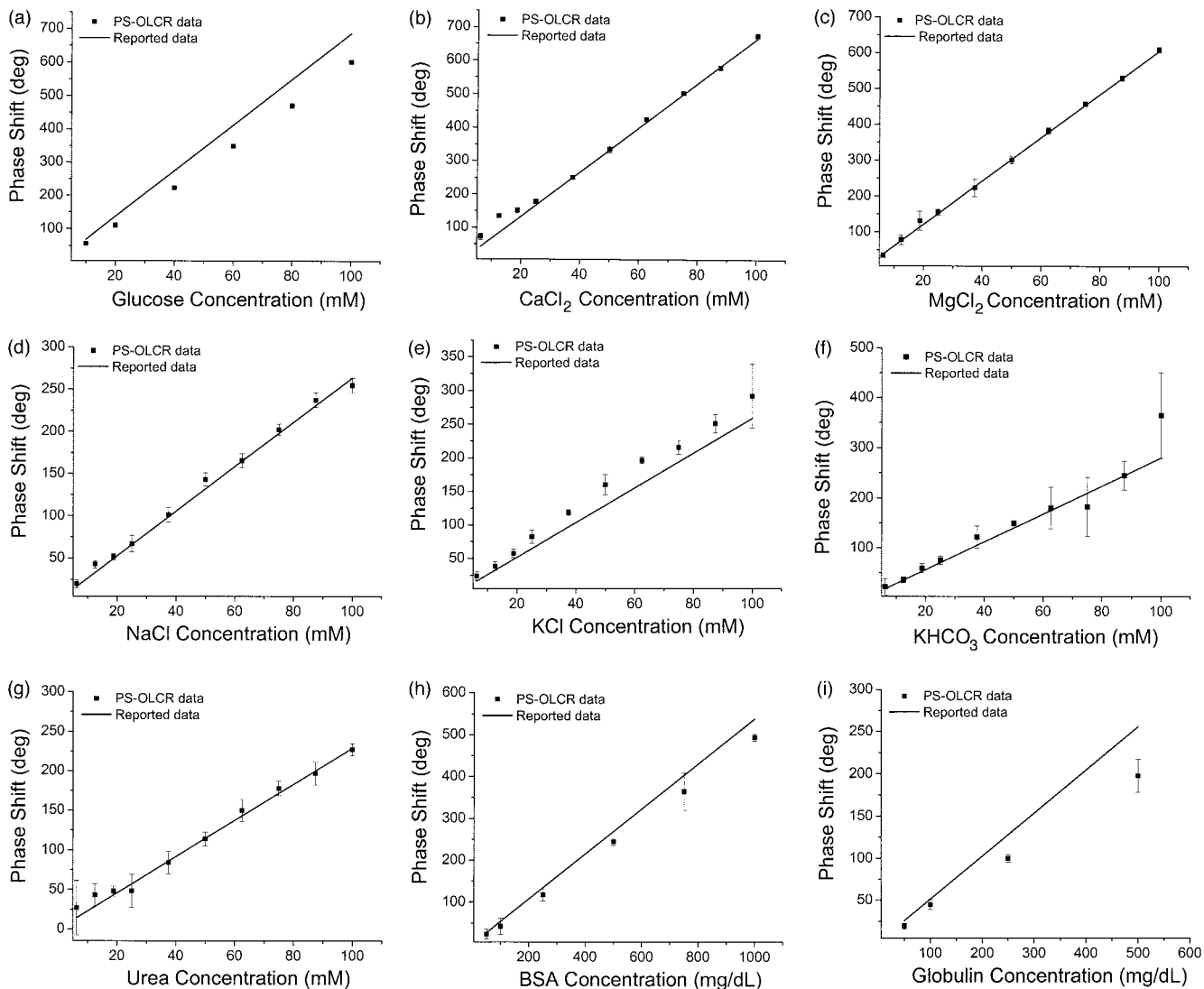


Fig. 3. Phase shift versus concentration of (a) glucose, (b)  $\text{CaCl}_2$ , (c)  $\text{MgCl}_2$ , (d)  $\text{NaCl}$ , (e)  $\text{KCl}$ , (f)  $\text{KHCO}_3$ , (g) urea, (h) BSA, and (i) globulin obtained from the PS-OLCR study in clear media (squares with SD bars) and from the literature (solid line).

#### 4. Discussion

The results shown in Figs. 3 and 4 demonstrate the capability of the PS-OLCR technique to detect small changes in the refractive index with a high degree of sensitivity. For instance, the phase difference between two phase-modulated signals for glucose and  $\text{KCl}$  shifted approximately 601 and 291 deg, respectively, in the range from 0 to 100 mM in the 485- $\mu\text{m}$ -thick cell. The small SD of the data points demonstrated in these studies (for example, glucose concentrations were measured with an average  $\text{SD} = \pm 0.7^\circ$  and  $\pm 11.7^\circ$  in clear and turbid media, respectively) demonstrate the high accuracy of the measurements. The higher SD observed in the experiments with the turbid media compared with that of the clear-media experiments resulted most likely from the decrease of the signal-to-noise ratio of the phase-modulated signal obtained from the back surface of the cell.

A summary of the observed changes in the phase

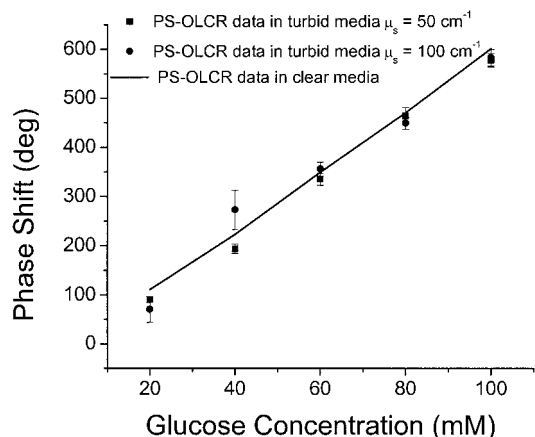


Fig. 4. Phase shift versus glucose concentration obtained in turbid media (aqueous suspension of polystyrene microspheres) with scattering coefficients similar to those of human tissues in the NIR spectral range: squares,  $\mu_s \cong 50 \text{ cm}^{-1}$ ; circles,  $\mu_s \cong 100 \text{ cm}^{-1}$ . The solid line shows PS-OLCR data obtained in clear media [see Fig. 3(a)].

**Table 1. Concentration-Dependent Changes in the Phase Shift and the Refractive Index for Major Analytes in the Body as Obtained from the Literature and Measured with the PS-OLCR Technique<sup>a</sup>**

Analyte	$\left[\frac{d\phi}{dC}\right]_{lit}$ (deg mM <sup>-1</sup> )	$\left[\frac{d\phi}{dC}\right]_{exp}$ (deg mM <sup>-1</sup> )	$\left[\frac{dn}{dC}\right]_{lit}$ (10 <sup>5</sup> mM <sup>-1</sup> )	$\left[\frac{dn}{dC}\right]_{exp}$ (10 <sup>5</sup> mM <sup>-1</sup> )	C <sub>physiol</sub> (mM)	$\Delta C_{physiol}$ $\times \left[\frac{dn}{dC}\right]_{exp}$ (10 <sup>5</sup> )
Glucose	6.85	5.89	2.55	2.20	3–30	59.23
CaCl <sub>2</sub>	6.66	6.43	2.48	2.39	2.1–2.6	1.20
MgCl <sub>2</sub>	6.04	6.08	2.25	2.26	0.7–1.0	0.68
NaCl	2.63	2.58	0.98	0.96	135–145	9.61
KCl	2.58	2.97	0.96	1.11	3.5–5	1.66
KHCO <sub>3</sub>	2.79	2.97	1.04	1.11	22–26	4.42
Urea	2.28	2.21	0.85	0.82	2.9–8.9	4.94
BSA*	0.54	0.50	0.20	0.19	0.35–0.45	0.019
Globulin*	0.51	0.40	0.19	0.15	0.26–0.41	0.022

<sup>a</sup>The table also shows the physiological range of analyte concentrations and the maximum possible effect on the refractive-index change. The  $d\phi/dC$  values for the listed analytes were obtained in a 485- $\mu$ m-thick cell. \* denotes that, for  $d\phi/dC$ ,  $dn/dC$ , and  $C_{physiol}$ , BSA and globulin are shown in deg dL mg<sup>-1</sup>, dL mg<sup>-1</sup>  $\times 10^{-5}$ , and mg dL<sup>-1</sup>, respectively.

shift and the refractive index for the analytes shown in Fig. 3 is presented in Table 1. Columns 2 and 3 show the concentration-dependent change in the phase shift found in the literature for  $\lambda = 436$  and 589 nm<sup>18,19</sup> and that experimentally measured with PS-OLCR ( $\lambda = 1.31 \mu\text{m}$ ), respectively. Corresponding dependencies of the refractive index on analyte concentration obtained from the literature and from experimental measurements are listed in columns 4 and 5, respectively. Normal reference laboratory values of the physiological changes in concentrations of these substances<sup>20</sup> are shown in the column 6. The last column shows the maximum possible influence of these substances on the refractive index in the physiological range. One can see from this table that (1) although the phase-shift changes that are due to changes in the refractive index are observed in all the studied analytes, the effect of glucose is greater compared with that of the other analytes and (2) the  $d\phi/dC$  (and  $dn/dC$ ) measured with PS-OLCR is generally slightly less at  $\lambda = 1.31 \mu\text{m}$  than that previously reported in the literature for the visible spectral range obtained with different optical approaches. This discrepancy is most likely due to the wavelength dependence of the refractive index. Nevertheless, the results shown in Fig. 3 and Table 1 suggest the capability of PS-OLCR to provide reliable, sensitive, and accurate measurements of the refractive indices as a function of analyte concentration.

To validate the experimentally measured dependence of the refractive index on glucose concentration, we used a conventional OCT system to study the dependence of OCT signal slope as a function of glucose concentration in an aqueous suspension of polystyrene microspheres. The principle of operation and the algorithm of mathematical processing of signals that were obtained with this conventional OCT system ( $\lambda = 1.3 \mu\text{m}$ ) were reported previously.<sup>8–10</sup> Figure 5 depicts the slope of the OCT signals obtained from an aqueous suspension of polystyrene microspheres versus the glucose concentration at 1.3  $\mu\text{m}$ .

Six glucose concentrations were measured in these experiments, ranging from 0 to 250 mM with a 50-mM increment. The SD is plotted as error bars. The calculated scattering coefficient is presented by the solid line. The calculation of the scattering coefficient was performed with Mie scattering theory, assuming  $dn/dC = 2.2 \times 10^{-5} \text{ mM}^{-1}$  (Table 1). One can see from this figure that the linear decrease of the OCT signal slope is in good agreement with the theoretically calculated decrease of the scattering coefficient with glucose concentration. Therefore the experimentally measured dependence of the refractive index on analyte concentration by use of PS-OLCR has been validated in this study.

We studied the capability of PS-OLCR to detect small changes in glucose concentration over the small range 0–10 mM. The experiment was performed in an aqueous solution of glucose in a cell with a thickness of 480  $\mu\text{m}$ , which is equal to that used in the previous experiments. Five concentrations of glu-

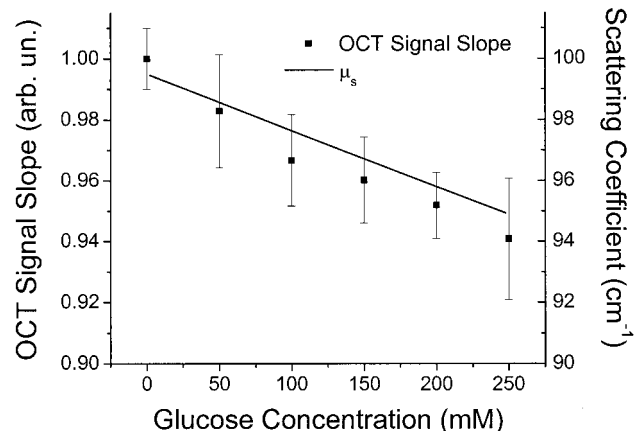


**Fig. 5. Slope of OCT signal (squares with SD bars) and scattering coefficient (line) calculated with the Mie theory of scattering versus glucose concentration in the aqueous suspension of polystyrene microspheres.**

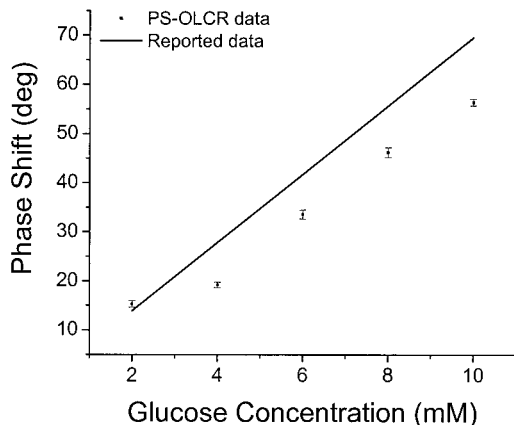


Fig. 6. Phase shift versus glucose concentration obtained from the PS-OLCR study over the small glucose-concentration range.

cose were measured, ranging from 2 to 10 mM (Fig. 6). The average SD obtained in this experiment was  $SD = \pm 0.76^\circ$ , similar to that found for large glucose concentrations [Fig. 3(a)]. Therefore the PS-OLCR technique is capable of measuring small glucose-induced changes in the refractive index with submillimolar resolution. These results suggest that the PS-OLCR method applied to the detection of glucose concentration has the level of accuracy that is required for clinical studies ( $\pm 1$  mM).

Temperature control of the sample under study is important in PS-OLCR measurements. Figure 7 demonstrates the dependence of the refractive index of water on temperature over the range from 0 to  $100^\circ\text{C}$ .<sup>18</sup> Evidently, small fluctuations in the sample temperature (e.g.,  $\pm 1^\circ\text{C}$ – $2^\circ\text{C}$ ) can reduce the accuracy of phase-shift measurements obtained with PS-OLCR. In our experiments we monitored the sample temperature by inserting a thermocouple in the cell near the measurement site. We found that because the temperature was nearly constant during the differential-phase measurements, we could ignore it during  $d\phi/dC$  and  $dn/dC$  calculations. Nev-

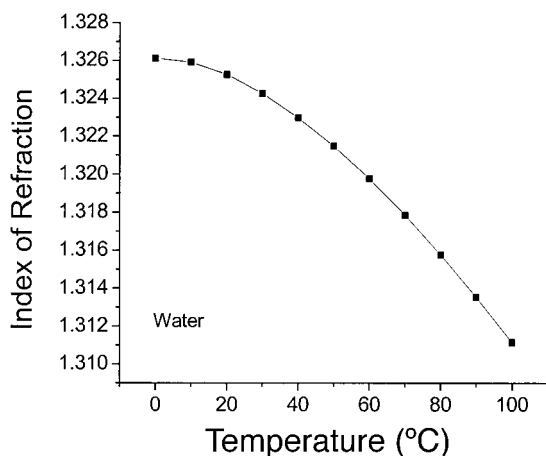


Fig. 7. Index of refraction of water as a function of temperature measured at  $\lambda = 1.01 \mu\text{m}$  (prominent spectral line of mercury). The data were obtained from Ref. 18.

ertheless, the temperature fluctuations in tissues should be monitored and accounted for during *in vivo* experiments, especially for long-term measurements.

## 5. Conclusion

We report the results of our theoretical and experimental pilot studies on the application of PS-OLCR to the noninvasive, sensitive, and accurate monitoring of analyte concentrations. The results obtained for aqueous solutions of glucose,  $\text{CaCl}_2$ ,  $\text{MgCl}_2$ ,  $\text{NaCl}$ ,  $\text{KCl}$ ,  $\text{KHCO}_3$ , urea, BSA, and globulin in clear and turbid media demonstrate (1) a good agreement between the refractive indices measured with the white-light refractometer and the PS-OLCR technique and those previously reported in the literature for the visible spectral range; (2) the effect of glucose on  $dn/dC$  is approximately 1–4 orders of magnitude greater than that of the other analytes at physiological concentrations; (3) a good agreement between the results obtained in translucent and scattering media, suggesting that PS-OLCR could be applied to *in vivo* measurements; and (4) a high (submillimolar) sensitivity of PS-OLCR for measurement of glucose concentrations.

We believe that PS-OLCR has the potential for use in the noninvasive, sensitive, and accurate monitoring of analyte concentrations both in clear and turbid media. Future studies will focus on *in vivo* tests of this technique in animals and humans. The influence of several potential obstacles on the sensitivity and specificity of the PS-OLCR method for *in vivo* monitoring of analyte concentrations in highly scattering tissues (e.g., birefringence of tissues, stability of specular reference points, and tissue temperature) will be addressed in future studies.

This research was supported in part by grant R21 NS40531 from the National Institute of Diabetes and Digestive and Kidney Diseases of the National Institutes of Health (NIH), by NIH grants R24 EY12877 and RR14069-02, and by Texas Advanced Technology Program grant ATP 3658-0357.

## References

1. D. Huang, E. A. Swanson, C. P. Lin, J. S. Schuman, W. G. Stinson, W. Chang, M. R. Hee, T. Flotte, K. Gregory, C. A. Puliafito, and J. G. Fujimoto, "Optical coherence tomography," *Science* **254**, 1178–1181 (1991).
2. J. M. Schmitt, "Optical coherence tomography (OCT): a review," *IEEE J. Sel. Top. Quantum Electron.* **5**, 1205–1215 (1999).
3. A. F. Fercher, W. Drexler, C. K. Hitzenberger, and T. Lasser, "Optical coherence tomography—principles and applications," *Rep. Prog. Phys.* **66**, 239–303 (2003).
4. C. K. Hitzenberger and A. F. Fercher, "Differential phase contrast in optical coherence tomography," *Opt. Lett.* **24**, 622–624 (1999).
5. D. P. Davé and T. E. Milner, "Optical low-coherence reflectometer for differential phase measurement," *Opt. Lett.* **25**, 227–229 (2000).
6. M. Sticker, K. Hitzenberger, R. Leitgeb, and A. F. Fercher, "Quantitative differential phase measurement and imaging in transparent and turbid media by optical coherence tomography," *Opt. Lett.* **26**, 518–520 (2001).

7. T. Akkin, D. P. Dave, T. E. Milner, and H. G. Rylander, "Interferometric fiber-based optical biosensor to measure ultra-small changes in refractive index," in *Optical Fibers and Sensors for Medical Applications II*, I. Gannot, ed., Proc. SPIE **4616**, 9–13 (2002).
8. R. O. Esenaliev, K. V. Larin, I. V. Larina, and M. Motamedi, "Noninvasive monitoring of glucose concentration with optical coherent tomography," *Opt. Lett.* **26**, 992–994 (2001).
9. K. V. Larin, M. S. Eledrisi, M. Motamedi, and R. O. Esenaliev, "Noninvasive blood glucose monitoring with optical coherence tomography: a pilot study in human subjects," *Diabetes Care* **25**, 2263–2267 (2002).
10. K. V. Larin, M. Motamedi, T. V. Ashitkov, and R. O. Esenaliev, "Specificity of noninvasive blood glucose sensing using optical coherence tomography technique: a pilot study," *Phys. Med. Biol.* **48**, 1371–1390 (2003).
11. T. Akkin, D. P. Davé, J. Youn, S. A. Telenkov, H. G. Rylander, III, and T. E. Milner, "Imaging tissue response to electrical and photothermal stimulation with nanometer sensitivity," *Lasers Surg. Med.* **33**, 219–225 (2003).
12. G. J. Tearney, B. E. Bouma, and J. G. Fujimoto, "High-speed phase- and group-delay scanning with a grating-based phase control delay line," *Opt. Lett.* **22**, 1811–13 (1997).
13. H. C. van de Hulst, *Light Scattering by Small Particles* (Dover, New York, 1981).
14. C. F. Bohren and D. R. Huffman, *Absorption and Scattering of Light by Small Particles* (Wiley, New York, 1983).
15. M. Bartlett and H. Jiang, "Measurement of particle size distribution in multilayered skin phantoms using polarized light spectroscopy," *Phys. Rev. E* **65**, 031906 (2002).
16. R. Bays, G. Wagnieres, D. Robert, J. F. Theumann, I. A. Vitkin, J. F. Savary, P. Monnier, and H. van den Bergh, "Three-dimensional optical phantom and its application in photodynamic therapy," *Lasers Surg. Med.* **21**, 227–234 (1997).
17. A. Wax, C. H. Yang, R. R. Dasari, and M. S. Feld, "Path-length-resolved dynamic light scattering: modeling the transition from single to diffusive scattering," *Appl. Opt.* **40**, 4222–4227 (2001).
18. D. Lide, *Handbook of Chemistry and Physics*, 82nd ed. (CRC Press, Boca Raton, Fla., 2001).
19. M. B. Huglin, *Light Scattering from Polymer Solutions* (Academic, New York, 1972).
20. A. Kratz and K. B. Lewandrowski, "Case records of the Massachusetts General Hospital. Weekly clinicopathological exercises. Normal reference laboratory values," *N. Engl. J. Med.* **339**, 1063–1072 (1998).